Analysis of multiple scattering from two-dimensional dielectric sea surface with iterative Kirchhoff approximation*

Luo Wei(罗 伟)[a], Zhang Min(张 民)[a]†, Zhou Ping(周 平)[b], and Yin Hong-Cheng(殷红成)[b]

[a] *School of Science, Xidian University, Xi'an* 710071, *China*
[b] *National Electromagnetic Scattering Laboratory, Beijing* 100854, *China*

(Received 3 December 2009; revised manuscript received 29 January 2010)

An iterative method in the Kirchhoff approximation is proposed for high frequency multiple electromagnetic scattering from two-dimensional dielectric sea surface. The multiple interaction of the scattering field is characterized with the corrected electromagnetic currents of the wind-driven sea surface. The actual surface currents are approximated with the iterative solution of the corrected currents. A newly developed sea spectrum, Elfouhaily spectrum, is utilized to build the sea surface model. The shadowing correction is improved by the Depth–Buffer algorithm. The validity of the iterative Kirchhoff approximation is verified by the agreement of backscattering coefficients with the measured data.

Keywords: sea surface, multiple scattering, iterative methods, shadowing correction

PACC: 4110H, 5235H, 9265M

1. Introduction

The study of the electromagnetic scattering from the sea surface is significant for remote sensing, surveillance and synthetic aperture radar (SAR) imaging of the ocean.[1] Many asymptotic methods in high frequency bands and numerical methods[2−9] have been developed recently. However, the two categories of methods both have drawbacks for sea surface scattering.[10]

The multiple scattering of sea surface, which arises from the roughness of wind wave has been studied with rationalistic analysis and experiment measurements.[11] The Neumann series solution for the second-kind magnetic field integral equation (MFIE) was also developed as a kind of iterative method for the perfectly electric conducting (PEC) rough surface.[12,13]

In the present paper, we propose an iterative Kirchhoff approximation (iterative KA) for the high frequency scattering of the wind-driven sea surface. The theoretical basis and formulations of the iterative procedure are expounded and illuminated with the surface current distribution in Section 2. Then the newly developed Elfouhaily spectrum is discussed and utilized for the sea surface modeling in Section 3, and a new shadowing correction is introduced with the help of Depth–Buffer technology in Section 4. The iterative method is verified by the measured data and two-scale method in Section 5. Finally, some concluding remarks are presented in Section 6.

2. Formulation of the problem

In order to reconcile the asymptotic methods with the numerical methods, the iterative KA is proposed to build a sea surface electromagnetic scattering model. The scattering from each surface realization is calculated, and the resulting scattering coefficients from all the realizations are averaged to obtain the Monte Carlo estimate results.

According to the Kirchhoff approximation,[1] the scattering field of the sea surface in the far zone is given as

$$\begin{aligned}\boldsymbol{E}^{\mathrm{s}}(\boldsymbol{r}) &= K\int[-\hat{k}_{\mathrm{s}}\times\boldsymbol{M}-\hat{k}_{\mathrm{s}}\times(\hat{k}_{\mathrm{s}}\times\boldsymbol{J})\eta]\\ &\quad\times\exp(\mathrm{j}\,\boldsymbol{k}_{\mathrm{s}}\cdot\boldsymbol{r}')\mathrm{d}s',\\ \boldsymbol{J} &= \hat{n}\times\boldsymbol{H},\\ \boldsymbol{M} &= -\hat{n}\times\boldsymbol{E},\end{aligned}\tag{1}$$

where $\boldsymbol{J}$ and $\boldsymbol{M}$ are the electric and the magnetic

*Project supported by the National Natural Science Foundation of China (Grant No. 60871070) and the National Pre-research Foundation and the Foundation of National Electromagnetic Scattering Laboratory, China.
†Corresponding author. E-mail: mzhang@mail.xidian.edu.cn
© 2010 Chinese Physical Society and IOP Publishing Ltd

surface currents respectively. Other parameters can be found in Ref. [1].

It is obvious that the accuracy of scattering field rests on the accurate determining of $\boldsymbol{J}$ and $\boldsymbol{M}$. Under the Kirchhoff approximation, the surface currents induced by the incident fields $\boldsymbol{E}^{\rm inc}$ and $\boldsymbol{H}^{\rm inc}$ are given as

$$\begin{aligned}\boldsymbol{J} &= \hat{n}\times\boldsymbol{H} = \hat{n}\times(\boldsymbol{H}^{\rm inc}+\boldsymbol{H}^{\rm r}),\\ \boldsymbol{M} &= -\hat{n}\times\boldsymbol{E} = -\hat{n}\times(\boldsymbol{E}^{\rm inc}+\boldsymbol{E}^{\rm r}),\end{aligned}\tag{2}$$

where $\boldsymbol{H}^{\rm r}$ and $\boldsymbol{E}^{\rm r}$ are the direct reflecting fields. Apparently equation (2) could interpret only the local scattering phenomenon.

In this paper we introduce the iterative solver with including the coupling scattering fields $\boldsymbol{E}_n^{\rm c}$ and $\boldsymbol{H}_n^{\rm c}$. Then the currents in Eq. (2) are substituted with

$$\begin{aligned}&\boldsymbol{J}_n = \boldsymbol{J}_0 + \hat{n}\times\boldsymbol{H}_n^{\rm c}(1+R_{v,h}),\\ &\boldsymbol{M}_n = \boldsymbol{M}_0 - \hat{n}\times\boldsymbol{E}_n^{\rm c}(1+R_{v,h}),\\ &n = 1,2,\ldots,N,\end{aligned}\tag{3}$$

where $\boldsymbol{J}_n$ and $\boldsymbol{M}_n$ are iterative solutions of the surface currents, while n denotes the iteration order. $R_{v,h}$ is the local reflection coefficient of the sea surface. The initial values of zeroth order $\boldsymbol{J}_0$ and $\boldsymbol{M}_0$ are actually the Kirchhoff approximation currents. And $\boldsymbol{E}_n^{\rm c}$ and $\boldsymbol{H}_n^{\rm c}$ are given as

$$\begin{aligned}\boldsymbol{E}_n^{\rm c}(\boldsymbol{r},\boldsymbol{r}') &= \int_S [-{\rm i}\,\omega\mu\boldsymbol{J}_{n-1}(\boldsymbol{r}')G(\boldsymbol{r},\boldsymbol{r}') - \boldsymbol{M}_{n-1}(\boldsymbol{r}')\times\nabla' G(\boldsymbol{r},\boldsymbol{r}')]{\rm d}s',\\ \boldsymbol{H}_n^{\rm c}(\boldsymbol{r},\boldsymbol{r}') &= \int_S [-{\rm i}\,\omega\varepsilon\boldsymbol{M}_{n-1}(\boldsymbol{r}')G(\boldsymbol{r},\boldsymbol{r}') + \boldsymbol{J}_{n-1}(\boldsymbol{r}')\times\nabla' G(\boldsymbol{r},\boldsymbol{r}')]{\rm d}s',\\ G(\boldsymbol{r},\boldsymbol{r}') &= \frac{\exp(-{\rm i}\,kR)}{4\pi R},\quad R = |\boldsymbol{r}-\boldsymbol{r}'|.\end{aligned}\tag{4}$$

Equation (4) is deduced from the Stratton–Chu equation and accounts for the multiple scattering of the sea surface. Although the integral in Eqs. (4) is improper, nevertheless, it is convergent for the Lyapunov surfaces. Since the depolarization due to the tilted facets of the rough sea surface occurs, the coupling field $\boldsymbol{E}_n^{\rm c}$ should be expressed with vertically polarized field $\boldsymbol{E}_{n,v}^{\rm c}$ and horizontally polarized field $\boldsymbol{E}_{n,h}^{\rm c}$. And $\boldsymbol{H}_n^{\rm c}$ is expressed with $\boldsymbol{H}_{n,v}^{\rm c}$ and $\boldsymbol{H}_{n,h}^{\rm c}$ for the same reason. Then equation (3) can be rewritten as

$$\begin{aligned}&\boldsymbol{J}_n = \boldsymbol{J}_0 + \hat{n}\times(\boldsymbol{H}_{n,v}^{\rm c}+\boldsymbol{H}_{n,h}^{\rm c}+\boldsymbol{H}_{n,v}^{\rm c}R_v+\boldsymbol{H}_{n,h}^{\rm c}R_h),\\ &\boldsymbol{M}_n = \boldsymbol{M}_0 - \hat{n}\times(\boldsymbol{E}_{n,v}^{\rm c}+\boldsymbol{E}_{n,h}^{\rm c}+\boldsymbol{E}_{n,v}^{\rm c}R_v+\boldsymbol{E}_{n,h}^{\rm c}R_h),\\ &n = 1,2,\ldots,N.\end{aligned}\tag{5}$$

Figure 1 shows the magnitude distributions of $\boldsymbol{J}_0$ and $\boldsymbol{J}_2$ on the sea surface. The currents are induced by 1-GHz incident wave and the wind speed is 5 m/s. In order to involve the multiple interactions between long-wavelength components, the length of sea surface geometrical model is ten correlation lengths of the sea surface. It is shown that $\boldsymbol{J}_0$ is evenly distributed on the sea surface and the rather periodic distribution of $\boldsymbol{J}_2$ is due to the regular surface fluctuation.

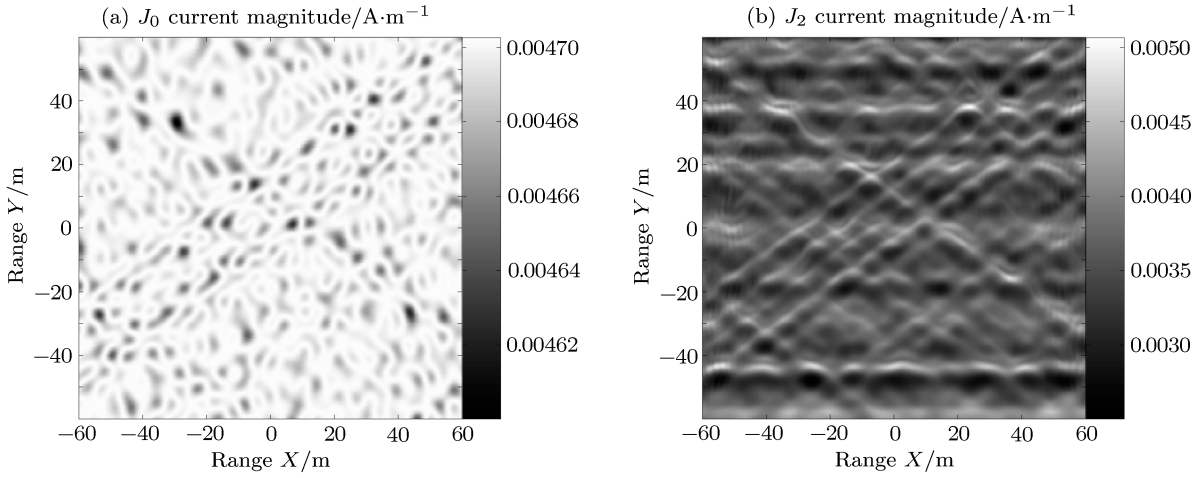


Fig. 1. Magnitude distributions of electric currents on 5 m/s sea surface, with the values of iteration order N being 0 (a) and 2 (b).

Moreover the magnitude range of $\boldsymbol{J}_0$ is much smaller than the one of $\boldsymbol{J}_2$. It can be concluded that the higher order currents provide more phase information resulting from the multiple interactions.

3. Sea spectrum

Recently there have been kinds of sea spectra such as Pierson spectrum, JONSWAP spectrum, Apel spectrum, and so on. Since these expressions of energy distribution satisfy the properties of ergodicity and stationarity, they have been widely used in the statistical simulation.

The Elfouhaily spectrum,[14] which was developed based on available field and wave-tank measurements and without any relation to remote-sensing data, is used to simulate the sea surface fluctuation. The Elfouhaily spectrum is no longer an empirical spectrum, but it is a fully-developed spectrum related only to the wind speed. Thus it is more suitable for the simulation of the sea surface. The general form of the Elfouhaily spectrum is given as

$$W(\boldsymbol{K}) = W(K,\psi) = W(K)G(K,\psi). \tag{6}$$

The directional spectrum $W(\boldsymbol{K})$, in which the wave vector is $\boldsymbol{K} = \hat{\boldsymbol{x}} \cdot K\cos\psi + \hat{\boldsymbol{y}} \cdot K\sin\psi$, contains nondirectional portion $W(K)$ and spreading function $G(K,\psi)$. The curvature spectrum $W(K)$ is composed of the spectra of low-wavenumber gravity waves and high-wavenumber capillary waves and given as

$$W(K) = (B_{\rm L} + B_{\rm H})/K^3. \tag{7}$$

The low-wavenumber curvature spectrum $B_{\rm L}$ and the high-wavenumber curvature spectrum $B_{\rm H}$ present the high-frequency and low-frequency portions of the spectrum energy respectively. And the realistic power spectrum of sea surface is anisotropic in the two-dimensional condition, thus the direction function is introduced[14]

$$G(K,\psi) = [1 + \Delta(K)\cos(2\psi)]/2\pi. \tag{8}$$

Figure 2 shows high-frequency and low-frequency portions of $B(K)$. The capillary wave $B_{\rm L}$ is sensitive to wave age Ω and contains less energy than the gravity wave spectrum $B_{\rm H}$, and $B_{\rm H}$ is affected by the wind speed in most frequency ranges.

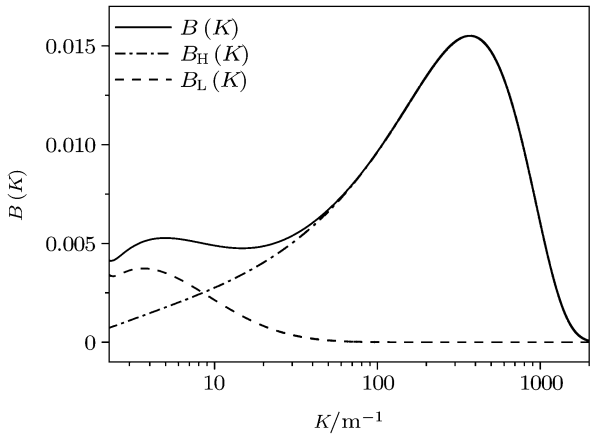


Fig. 2. Portions of predicted curvature spectrum $B(K)$.

4. Shadow correction

For the sake of high-frequency limitation, some regions of the rough surface may be shielded by parts of the surface. In this paper, the shadow correction of the sea surface is made based on the Depth–Buffer algorithm.[15] The principle of the Depth–Buffer correction process is given as follows.

The rough surface is located in the Cartesian coordinate system and each facet of the rough surface is projected onto a projection plane which is perpendicular to incident direction (θ,φ). The projection plane is defined as follows:

$$\begin{cases} \hat{x}' = -\sin\varphi\ \hat{x} + \cos\varphi\ \hat{y}, \\ \hat{y}' = -\cos\theta\cos\varphi\ \hat{x} - \cos\theta\sin\varphi\ \hat{y} + \sin\theta\ \hat{z}, \\ \hat{z}' = \sin\theta\cos\varphi\ \hat{x} + \sin\theta\sin\varphi\ \hat{y} + \cos\theta\ \hat{z}. \end{cases} \tag{9}$$

The z' value of the model projection which is stored in the depth buffer represents the distance from the facet to the observer. Then the projection plane is subdivided into pixels of which the number is more than the one of the facets on the sea surface. If the projections of two facets are overlapped, the two facets are shadowed by each other. According to the value z' of the projections, we can determine which facet is shadowed in the view direction. The shadow area can be calculated by the number of the overlapped pixels. The facets which are shadowed in the incident direction or the scattering direction make no contribution to the scattering field. Thus these facets should be removed from the integral in Eq. (1).

Different from the correction function of scattering coefficient, the Depth–Buffer shadow correction

examines each facet on the concrete surface whose scattering field can be calculated.

5. Numerical results and discussion

According to the linear accumulative theory, wind-driven sea surfaces are modeled based on the Elfouhaily omnidirectional spectrum as shown in Fig. 3.

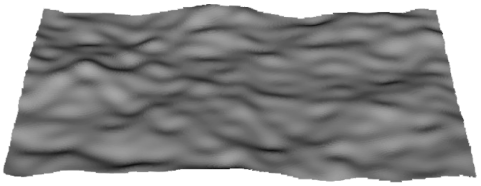


Fig. 3. Sea surface model based on the Elfouhaily spectrum.

Fifty realizations are simulated for each calculation based on the principle of the Monte Carlo method. According to Section 2, the iteration number is significant for the accuracy in determining the corrected surface current. Moreover the scattering coefficient tends to be convergent with the increase of the iteration order N. Since the iterative KA is a high frequency method based on KA, the edge effect can be neglected for the electrically large two-dimensional sea surface.

In order to verify the accuracy of the iterative KA, the numerical results of sea surface backscattering are shown in Fig. 4, where the sea surfaces with relative dielectric constant (32.349644, 36.615556) is illuminated, with using a 14-GHz incident wave. It can be seen that the numerical results of the iterative KA are consistent well with the measured data.[16] Compared with the result obtained by the two-scale method (TSM),[17] the oscillation of iterative KA originates from the realistic fluctuation of sea surface, which is similar to the numerical result. It is obvious that the scattering power from the normal direction is stronger than the one at large scattering angles, since the normal scattering is identical to the specular scattering. The VV polarization is higher than the HH one, as the absorption of the V polarized wave by sea water is stronger than that of the H polarized wave. It should be noted that the numerical result of the traditional TSM is just the scattering coefficient, while the iterative KA is able to provide the scattering field which can be used in the composite scattering from targets on the sea surface.

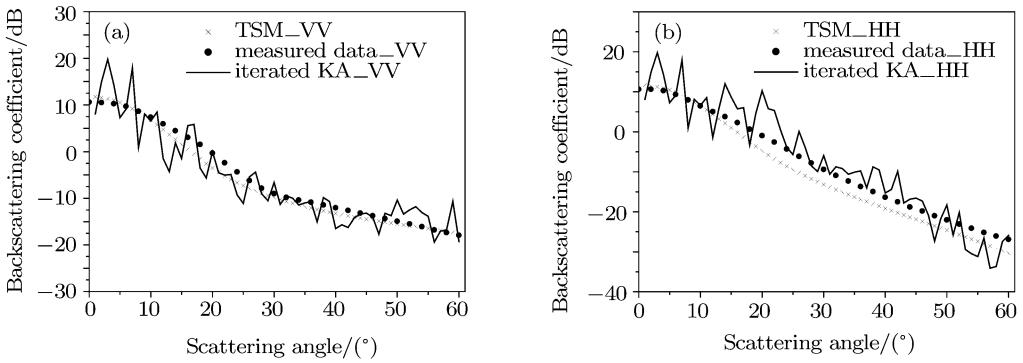


Fig. 4. Comparisons of backscattering coefficients calculated by different methods. (a) VV polarized, (b) HH polarized.

The bistatic scattering of the sea surface is shown in Fig. 5. The frequencies of the incident wave are 1 GHz and 10 GHz in Fig. 5(a) and Fig. 5(b) respectively. The wind speed is 15 m/s and the dielectric constant is the same as that in Fig. 4. In order to analyse the bistatic scattering, different incident directions are used in Fig. 5 but the scattering angle keeps consistent with the incident angle. As shown in Fig. 5(a) for the different incident azimuthal angles the scattering power strengths reach their maximum values in the specular direction, but reach their minimum values on the plane orthogonal to the specular plane. The scattering in the specular direction is termed the coherent scattering, due to its predictable, and constant, phase relative to that of the incident wave. The off-specular scattering, termed incoherent scattering, is caused by the surface roughness and is the source of the sidelobes. It can be seen that the coherent scattering is the main contribution of the sea

surface scattering. Figure 5(b) shows that the scattering power reduces with the increase of the distance from the specular direction, and the peak in the specular direction is more prominent at a larger incident angle. This proves that the sea surface is rougher at a large incident angle than at a small one in terms of the radar wave length, since more energy is diffused by the rougher surface.

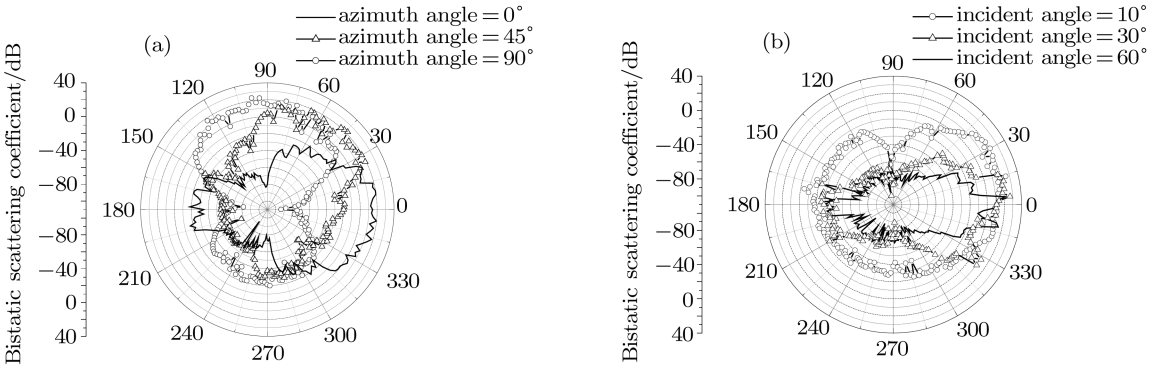


Fig. 5. Bistatic scattering coefficients versus scattering azimuth angles. In panel (a), the incident angle is 30°, and the incident azimuth angles are 0°, 45° and 90°, respectively. In panel (b), the incident azimuth angle is 0°, and the incident angles are 10°, 30° and 60° separately.

6. Conclusion

A new approach to the multiple scattering of the large two-dimensional sea surface is proposed. The iterative KA is actually a compromise between the numerical method and the asymptotic approximation method, thus the calculating of efficiency advances markedly. Moreover the limitation to the operating frequency is relaxed based on the Kirchhoff approximation. The validity of the method is verified by the agreement of the iterative KA with the two-scale method and the measured data. The electromagnetic currents show that the contribution of the intensity from multiple scattering becomes significant with the increase of root mean square height of the roughness and the angle of oblique incidence. It is concluded that the Depth–Buffer technology eliminates the self-shadowing effectively. Though the accuracy of the iterative KA is equivalent to the one of the TSM, the field provided by the iterative KA is more practical for the composite scattering and the SAR technology.

References

[1] Ulaby F T, Moore R K and Fung A K 1982 *Microwave Remote Sensinz* Vol. 2 (London: Addison-Wesley) p. 295
[2] Liu Y, Wei E B, Hong J L and Ge Y 2006 *Chin. Phys.* **15** 2175
[3] Li Z J, Xiong Y S and Liu Z L 1997 *Chin. Phys.* **6** 731
[4] Guo G J, Su L and Bi S W 2005 *Acta Phys. Sin.* **54** 2448 (in Chinese)
[5] Liu C X, Cheng C F, Ren X R, Liu M, Teng S Y and Xu Z Z 2004 *Acta Phys. Sin.* **53** 427 (in Chinese)
[6] Pinel N, Johnson J T and Bourlier C 2009 *IEEE Trans. Antennas Propag.* **57** 546
[7] Inan K and Ertürk V B 2006 *IEEE Trans. Geosci. Remote Sens.* **44** 3320
[8] Huang S X, Zhao X F and Sheng S 2009 *Chin. Phys.* B **18** 5084
[9] Wei E B and Ge Y 2005 *Chin. Phys.* **14** 1259
[10] Warnick K F and Chew W C 2001 *Waves in Random and Complex Media* **11** R1
[11] Hsieh C Y and Fung A K 2005 *Progress in Electromagnetics Research* **54** 199
[12] Holliday D 1987 *IEEE Trans. Antennas Propag.* **35** 120
[13] West J C and Sturm J M 1999 *IEEE Trans. Antennas Propag.* **47** 1281
[14] Elfouhaily T, Chapron B, Katsaros K and Vandemark D 1997 *J. Geophys. Research* **102** 15781
[15] Okino N, KaKazu Y and Morimoto M 1984 *IEEE Computer Graphics and Applications* **4** 79
[16] Arnold-Bos A, Ali K and Martin A 2007 *IEEE Trans. Geosci. Remote Sens.* **45** 3372
[17] Bass F G and Fuks I M 1979 *Wave Scattering from Statistically Rough Surfaces* (Oxford: Pergamon Press) p. 418